

## Article

# The Influence of Fibres on the Properties and Sustainability of Oil-Impacted Concrete

Fahad Aljuaydi <sup>1,\*</sup>, Rajab Abousnina <sup>2,\*</sup>, Omar Alajarmeh <sup>3</sup> and Abdalrahman Alajmi <sup>4</sup> 

<sup>1</sup> Department of Mathematics, College of Sciences & Humanities, Prince Sattam Bin Abdulaziz University, Al-Kharj 11942, Saudi Arabia

<sup>2</sup> School of Civil and Mechanical Engineering, Curtin University, Perth 6102, Australia

<sup>3</sup> Centre for Future Materials (CFM), University of Southern Queensland, Toowoomba 4350, Australia; omar.alajarmeh@unisu.edu.au

<sup>4</sup> Department of Mechanical and Aerospace Engineering, University of Strathclyde, Glasgow G1 1XJ, UK; abdalrahman-r-e-s-r-alajmi@strath.ac.uk

\* Correspondence: f.aljuaydi@psau.edu.sa (F.A.); rajab.abousnina@curtin.edu.au (R.A.)

**Abstract:** There are significant environmental and health consequences associated with oil-contaminated sand due to its toxic and persistent nature. The impacts include disrupted ecosystems with harm to plants and animals and contamination of water sources, requiring immediate and sustained remediation. Using oil-contaminated sand in construction addresses waste management and promotes sustainability by reducing waste, protecting the environment, saving energy, and driving innovation. This study investigates the impact of crude oil-contaminated sand on concrete's physical and mechanical characteristics. It focuses on assessing the impact of incorporating four different fibres (Forta Ferro PP, ReoShore 45 PP, glass, and steel fibres) and finding the optimal quantity (0.1, 0.2, 0.3, 0.4 or 0.5%) to improve the physical and mechanical properties of concrete prepared with sand contaminated by crude oil. The impact of crude oil on the bond strength between fibres and concrete was examined. Additionally, the effect of crude oil on heat flow and cumulative heat was analysed. The results demonstrated that increasing oil content decreases concrete density and compressive strength. Nevertheless, the findings indicated that sand contaminated with 10% oil is suitable for low-strength concrete applications. Incorporating 0.1% of Forta Ferro PP, glass, and ReoShore 45 PP fibres had a negligible impact on the mechanical properties of concrete contaminated with 10% oil. Comparatively, steel fibres enhanced the concrete's compressive strength by 30% at 0.1%, and the flexural strength improved by 9.6% at 0.5%. Concrete with a 10% crude oil content reinforced with steel fibres hinders fracture stabilisation and load transfer, making it suitable as a sustainable material for low-strength civil engineering applications.

**Keywords:** sustainable materials; short fibres; oil contamination; mechanical properties; crude oil; civil engineering applications



**Citation:** Aljuaydi, F.; Abousnina, R.; Alajarmeh, O.; Alajmi, A. The Influence of Fibres on the Properties and Sustainability of Oil-Impacted Concrete. *Sustainability* **2024**, *16*, 7344. <https://doi.org/10.3390/su16177344>

Academic Editor: Tim Gray

Received: 18 July 2024

Revised: 13 August 2024

Accepted: 19 August 2024

Published: 26 August 2024



**Copyright:** © 2024 by the authors. Licensee MDPI, Basel, Switzerland. This article is an open access article distributed under the terms and conditions of the Creative Commons Attribution (CC BY) license (<https://creativecommons.org/licenses/by/4.0/>).

## 1. Introduction

Worldwide energy consumption is predicted to rise by 37% by 2040 due to increased oil consumption in the transport and petrochemical sectors [1]. The demand of 90 million b/d in 2013 is expected to rise to 104 mb/d by 2040, highlighting the increasing dependence on oil as a primary energy source [2,3]. Throughout the upcoming 25 years, the world is expected to continue to rely on fossil fuels for a minimum of 50% of its power generation, even with the anticipated growth of wind and solar energy [4,5]. The proportion of each energy source in the total final fuel consumption is shown in Figure 1. The figure shows that oil is the most sought-after energy source, accounting for more than forty percent of global energy consumption. Hydrocarbon pollution in soils has become a significant environmental concern worldwide, primarily due to the extensive use of oil as an energy source [6,7]. This pollution can arise from various sources, including oil spills, leakage

from underground storage tanks, industrial discharges, and improper disposal of oil and oil-based products [8]. The effects are multifaceted, affecting the surrounding sand's physical, chemical, and biological properties, which results in significant environmental and ecological impacts [9].

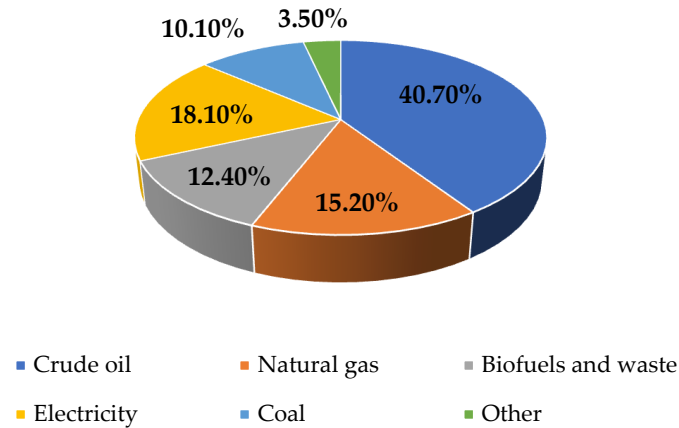


**Figure 1.** Energy-source-specific final fuel usage shares [3].

In Asia, an estimated 6.7 M Bbls of crude oil was spilt in the deserts of Arabia, Persia, and Kuwait in 1991, leading to substantial contamination. This intentional release of material impacted about 700 km of coastline stretching from Kuwait to Saudi Arabia and a small area in the Kuwaiti desert. A BP deepwater horizon drilling rig incident in 2010 resulted in a total leakage of 91 million L of oil in the Gulf of Mexico. This spill had a significant impact on around 110 km of Louisiana coastline. In Africa, the Niger Delta experiences leakage of more than 38 million L of crude oil each year. The leading causes of these spills are unknown factors (31.85%), third-party actions (20.74%), and mechanical failures (17.04%) [10,11]. Oil pollution in the Niger Delta has not only affected soil but also residents' health due to ingestion and inhalation of and contact with crude oil constituents, potentially leading to acute and long-term health issues [4]. In 2008, the VEBA (Vereinigte Elektrizitäts- und Bergwerks-AG) Oil Operation (Tripoli, Libya) discharged 71 million L of crude oil as a preventive measure to avoid an explosion in a tank caused by human error during maintenance [12,13]. Figure 2 shows crude oil contamination in Libyan oil fields caused by pipeline oil leakage and oily wastewater.



**Figure 2.** Crude oil contamination, Libya, 2024.

In 2009, an extensive oil spill contaminated around 60 km of beaches on Moreton Island in Australia, causing significant damage to the greatest wetland area in the region. These crude oil catastrophes are primarily caused by deteriorating infrastructure, inadequate upkeep, and human fallibility [14]. Various methods exist for remedying soils polluted by petroleum hydrocarbon (PHC) contamination. These procedures include conventional techniques, such as excavating and disposing of the impacted soil in designated landfills, placing protective covers over the polluted portions at the site, and stabilising the soil using chemicals like lime, apatite, and cement. Moreover, the use of chemical techniques like bioremediation is a possibility. The prohibitive expense of treatment technologies and the dumping of treated materials in landfills without any potential future uses make the existing techniques for addressing polluted soils unviable [9].

Using oil-contaminated sand in construction reduces waste disposal and promotes a circular economy by transforming waste into valuable resources. This strategy lowers building projects' environmental footprint and mitigates oil pollution's effects on ecosystems [15]. By immobilising contaminants within the concrete, the risk of leaching and environmental contamination is minimised, supporting ecological sustainability [16,17]. Reusing contaminated sand in construction reduces energy-intensive processing and lowers the demand for extracting and transporting virgin sand, which involves high energy consumption and carbon emissions. Recycling materials in construction leads to substantial energy savings and decreased greenhouse gas emissions. Additionally, recycled materials often cost less than new, virgin materials, making sustainable construction more affordable and financially feasible [18]. Previous studies [19,20] have investigated using sand contaminated with crude oil in concrete as a potential solution for contaminated sand, contributing to a cleaner environment and cost-effectiveness in the construction industry. However, previous studies have found that sand contaminated with crude oil can negatively impact concrete's mechanical properties, reducing its compressive strength [21,22]. Recent research studies [13,23] found that cement mortar with 1% light crude oil contamination achieved the highest compressive strength at 28 days, 17% higher than that of uncontaminated samples. However, adding more than 2% crude oil reduces strength gradually. As a result of this decrease in strength, concrete that has been affected by high percentages of crude oil is often only suitable for non-load-bearing constructions, such as concrete blocks and grout concrete [13,24].

Adding fibres to oil-impacted concrete can be an effective strategy to counteract the decrease in concrete strength. Fibres can improve the mechanical properties of concrete, including its compressive, tensile, and flexural strength, by enhancing its internal structure [25,26]. Strengthening the internal structure and improving the mechanical properties of oil-contaminated concrete with fibres can restore its performance and make it suitable for various construction applications [26,27]. Proper selection, mixing, and quality control are key to achieving the desired benefits from fibre reinforcement. Hence, adding fibres to oil-impacted concrete may mitigate the decrease in strength. Concrete is recognised as a somewhat fragile substance when exposed to typical stresses and impact loads, with its tensile strength only about one-tenth of its compressive strength. Fibres are introduced to improve concrete's mechanical characteristics and behaviour in its many uses. Therefore, incorporating fibres into concrete affected by high oil contamination may compensate for the known reduction in concrete strength. Fibres are proposed to improve concrete's mechanical properties and performance in various applications. Fibre-reinforced concrete (FRC) can improve impact resistance, abrasion resistance, durability, vibration tolerance, and (mainly) crack-control properties [28]. Fibres are often discontinuous and randomly dispersed inside a cement matrix. Construction sector materials exhibit diversity in kinds, shapes, characteristics, and availability [29,30]. This study addresses a critical research gap regarding the impact of fibres on the properties and sustainability of concrete containing oil-contaminated sand. It investigates the synergy between the impact of incorporating crude oil into concrete and how utilising four different types of fibres affects the enhancement of the mechanical properties of

concrete, mainly when using up to 10% oil-contaminated sand. The research examines how this level of oil contamination affects the mechanical and physical properties of concrete and evaluates the effectiveness of various fibres in mitigating these impacts. The study aims to develop sustainable construction materials that address ecological waste challenges while ensuring that concrete remains suitable for structural applications. This research is pivotal for advancing sustainability in the construction industry by demonstrating how waste materials can be repurposed effectively without compromising performance standards.

## 2. Materials

### 2.1. Aggregate

A sieve analysis was conducted, and the sand particles were found to be smaller than 2.36 mm [31]. Fine sand particle size distribution (PSD) was performed based on AS 1141.11.1-2009 [32]. Oil was mixed into the dry sand three days before casting to ensure a uniform level of oil contamination, accurately simulating real-world contaminated sand conditions (Figure 3). The aggregate was submerged in water for one day before casting to attain a saturated surface dry (SSD) state. The Australian Standard details the procedures for choosing the aggregate for the study's trials (AS 1726-1994) [33].

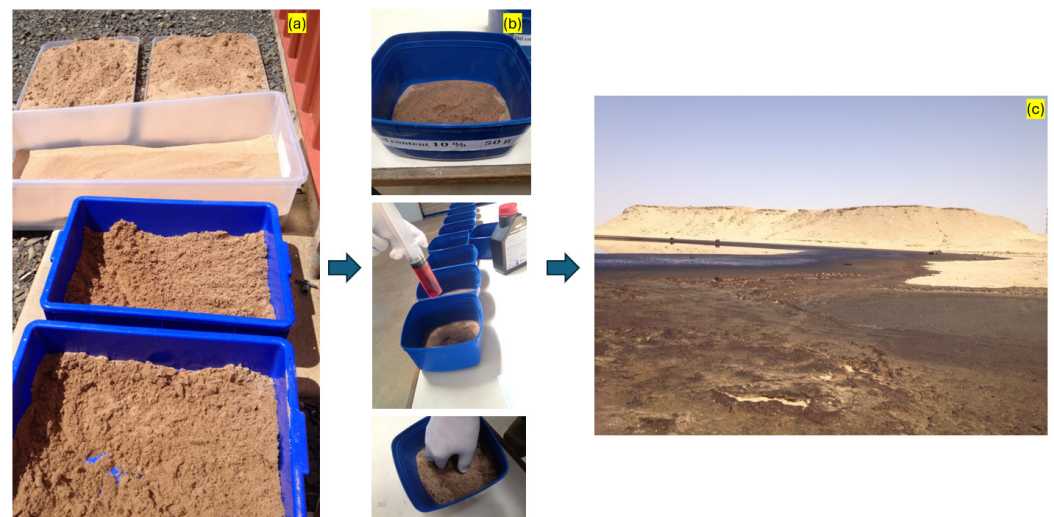


**Figure 3.** Sample preparation of oil-contaminated sand: (a) dried sand; (b) mixing oil with sand; (c) actual oil-contaminated sand (oil field, Libya, 2024).

### 2.2. Light Crude Oil

Light crude oil, characterised by its low density and high API gravity, can be readily refined into gasoline and diesel because of its low viscosity and high yield. In this study, mineral Fork w2.5 motorcycle oil was used. This oil was chosen because it is risk-free to use in the laboratory and comparable to light crude oil [34].

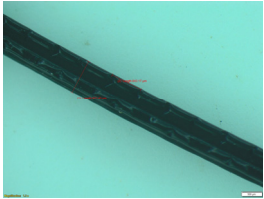
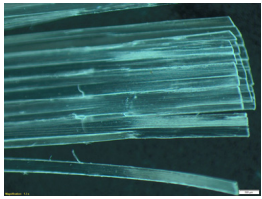
### 2.3. Cement

GP, which stands for general-purpose cement, was used.

### 2.4. Fibres

This study evaluated the effects of 4 different kinds of fibres. All types of fibres differ in properties such as material, strength, and geometry [25]. The properties of the fibres used in this study are outlined in Table 1.

**Table 1.** Polymeric and non-polymeric fibre properties used in this study [25].

Type of Fibre	Forta Ferro	ReoShore 45	Glass Fibres	Steel Fibres
Material	100% virgin copolymer/polypropylene	100% virgin copolymer/polypropylene (high-performance polypropylene geotextile)	Virgin homopolymer polypropylene	Bright low-carbon steel wire
Form	A twisted bundle of non-fibrillated monofilaments	Monofilament fibre system	Collated fibrillated fibre	Round wire, hooked shape
Fibre Count	161,900/kg	31,000/kg		15,318/kg
Length	38 mm	45 mm	19 mm	35 mm
Estimated Diameter	0.8 mm	0.8 mm		0.55 mm
Specific Gravity	0.91	0.8 mm	0.91	2.4 mm
Tensile Strength	570–660 MPa	0.91	570–660 MPa	2.5 mm
Melting Point	160 °C	Excellent		7.93
Colour	Grey	750–850 MPa	White	1250–1350 MPa
				

## 2.5. Mix Design

### 2.5.1. Concrete Mix Design

A mix design with a 3:3:1 ratio and a water-to-cement ( $w/c$ ) ratio of 0.5 was used [23].

### 2.5.2. Characteristics of Oil-Contaminated Concrete

The initial stage investigated the physical and mechanical properties of concrete prepared with oil-contaminated sand (0, 1, 2, 6, 10, and 20% by dry volume of sand), including the compressive strength. The first study's primary objective was to determine the maximum amount of oil that can be considered as a sustainable material suitable for construction and buildings.

### 2.5.3. Properties of Oil-Impacted Concrete with Fibres

The second stage examined how fibres influence concrete's physical and mechanical properties when incorporated with oil-contaminated sand (see Table 2). The concrete made with the maximum oil content deduced from the first stage was subjected to compressive and flexural forces, with four kinds of fibres examined (Forta Ferro PP, ReoShore 45 PP, glass, and steel fibres). A 0.1% by volume quantity of concrete was used for the comparative study, as this was the lowest recommended amount for polypropylene fibres among the four types. This stage aimed to identify the fibre type that significantly enhances the mechanical properties of concrete with 10% crude oil contamination.

**Table 2.** Second-stage tests.

Test	Type of Fibre	Fibre Quantity	
		% by Volume	kg/m <sup>3</sup>
Compression	Forta Ferro PP	0.1	0.91
	ReoShore 45		0.91
	Polypropylene		0.91
	Steel		7.93
Flexural	Forta Ferro-PP	0.1	0.91
	ReoShore 45		0.91
	Polypropylene		0.91
	Steel		7.93

#### 2.5.4. Fibre Dosage for Oil-Impacted Concrete

The third stage investigated the best-performing fibre determined from the second stage at a range of dosage amounts (Table 3). Quantity rates were guided by the recommended quantity for the most effective fibre according to the literature, with a recommended range of 15 to 30 kg/m<sup>3</sup> for steel fibres. As per McKee's theory, the minimal fibre dose allowed is essential to achieve a maximum average spacing factor of 0.45 times the fibres' nominal length [35]. Based on McKee's theory, the steel fibre dosage was set at a minimum of 16.71 kg/m<sup>3</sup>. The theory also specifies that fibres should not be spaced more than 0.45 times the total length [36]. This stage aimed to ascertain the ideal fibre quantity that enhances the concrete's mechanical properties.

**Table 3.** Final stage test outline.

Test	Type of Fibre	Fibre Quantity	
		% by Volume	kg/m <sup>3</sup>
Compression	Steel	0.1	0.9
		0.2	15.86
		0.3	23.79
		0.4	31.72
Flexural	Steel	0.1	0.9
		0.2	15.86
		0.3	23.79
		0.4	31.72

#### 2.6. Preparation of Specimens

This study used 100 × 200 mm cylindrical plastic moulds and 100 × 100 × 300 mm square prism moulds, glad wrap for cast specimens, and curing chambers used at 25 °C and 85% humidity. A slump test was conducted to see the impact of fibre dosages on the workability of the oil-contaminated concrete (Figure 4).

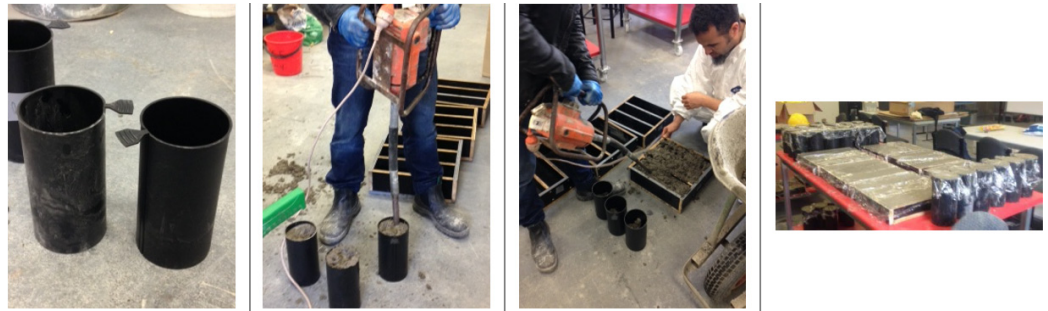


**Figure 4.** Concrete casing (plastic moulds and vibrator).

### 2.7. Compressive Strength

Compression testing complied with the ASTM [37] guidelines for the standard test procedure for determining the compressive strength of cylindrical concrete specimens. The test technique subjects moulded cylinders to a compressive axial force at a predetermined rate of (1.5 mm/min) until the specimen breaks.

### 2.8. Flexural Strength Test

The test was conducted based on ASTM C1609 [38]. The test method uses a four-point loading system on a supported beam to assess the parameters which are derived from the load–deflection curve to further evaluate the flexural performance of fibre-reinforced concrete. The modulus of rupture formula is used to calculate both the initial peak load and the subsequent peak loads, along with the associated stresses [38].

### 2.9. Isothermal Calorimetry Test (Hydration Test)

A Tam Air isothermal calorimeter was used to measure heat evolution during the hydration process, which complied with C1679-22 [1]. The pastes were mixed, sealed in ampules, and kept under isothermal conditions for 72 h at 25 °C. Salt was used as a reference material in the reference chamber to compare and calibrate heat evolution measurements. The heat of the hydrated cement was calculated by integrating the area under the heat flow curve. The total heat released during the hydration process was quantified, providing insights into the overall heat generation characteristics of the materials.

### 2.10. Workability Test

The workability of freshly prepared concrete with different percentages of fibres was assessed right after mixing the concrete.

### 2.11. Microscope Observation

The interior sections of the specimens were imaged using a microscope set to 65× magnification and analysed immediately after the compression test (28 days).

## 3. Results and Discussion

### 3.1. Impact of Crude Oil on Compressive Strength

Figure 5 visually depicts the data for the compressive failure load. The average strength of compression specimens free from contamination was 24.5 N/mm<sup>2</sup>. The compressive strength decreased in proportion to the rise in crude oil contamination. However, in this case, an oil content of 1% resulted in a 4% increase in strength, leading to an average compressive strength of 25.5 N/mm<sup>2</sup>. The oil likely contributed to this increase by enhancing the concrete's adhesion. The combination of oil and concrete significantly enhanced the sand's resistance to separation while simultaneously minimising water seepage. Recent research identified that sand tainted with 1% of crude oil obtained an ideal sand cohesiveness of 10.76 kN/m<sup>2</sup> [23].

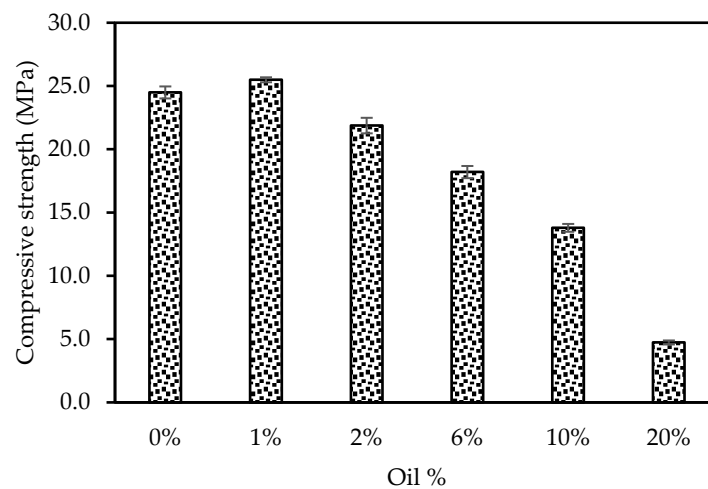


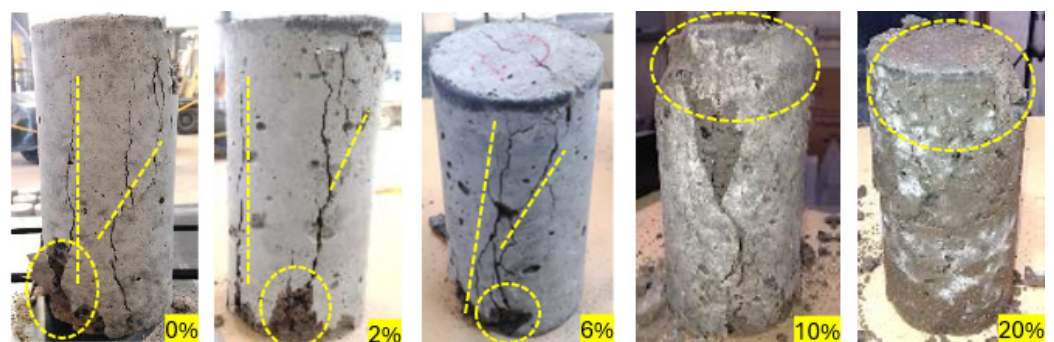
**Figure 5.** Mean compressive strength with different oil concentrations.

According to this study, when the oil content exceeds 1%, the sand becomes oversaturated, and the compressive strength of concrete significantly decreases at high percentages. In comparison with the uncontaminated samples, the strength of concrete decreased by 10.7%, 25.7%, 43.7%, and 80.7% for sand with an oil content of 2%, 6%, 10%, and 20%, respectively. Previous studies [19,39] found that oil has a negative effect on the mechanical properties of standard cement concrete. These studies induced that oil obstructs the development of bonds between mortar and aggregate, primarily due to the oil particles coating the sand grains.

The effective surface area for bonding with mortar reduces once aggregates reach a saturation state just before surface air drying (SSD). A film of moisture, consisting of a barrier of liquid oil, covers the individual aggregates, reducing their surface area. The film, called the water film thickness, lubricates the sand particles that slide past each other, and this dissolved water enables weaker binding between particles [40,41]. As the film's oil content and viscosity increase, cohesion between aggregates diminishes, causing additional particle slippage. When the oil leaches out, air voids result in a cement paste that is relatively porous with decreased internal strength. This porosity determines the decisive compressive strength of the concrete.

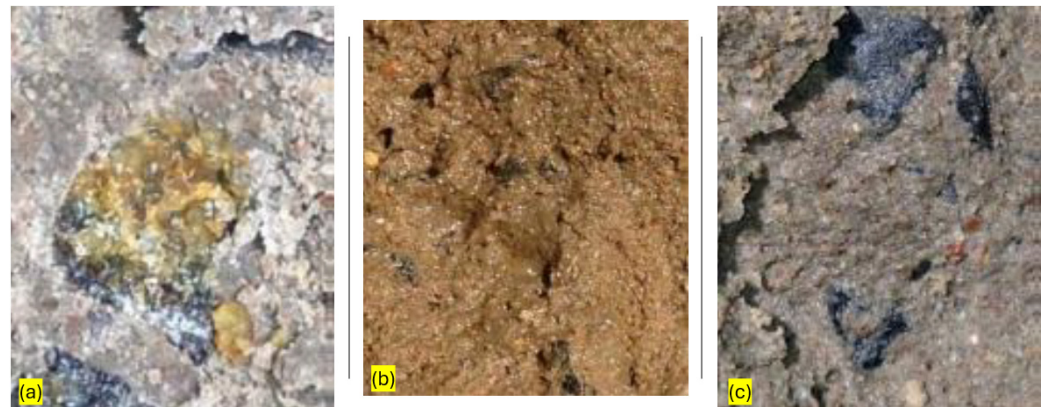
### 3.2. Failure Behaviour of Oil-Impacted Concrete

Figure 6 displays the failure modes for various mix designs. Conical and splitting failures were the most common. Cylinders with caps made of unbonded neoprene rarely failed in a conical manner. This was probably due to the tremendous variability in the construction of neoprene caps. Fractures usually start at the bottom cap and propagate across the cylinder, perpendicular to the applied load [37].



**Figure 6.** Splitting failure of specimens containing different percentages of oil.

The specimens started to fail at the top because of crushing. This was seen in all the specimens with 10% oil contamination and even more so when it reached 20%. In both the 6% and 10% contamination specimens, excess oil was found settled within the specimens (Figure 7a,b). This excess oil in the 10% contaminated specimen was less visible due to the high oil saturation level within the specimen. Instead, oil appeared more as a liquid in the indentation formed by the aggregate in the 20% contamination specimen. Oil was crystallised in the 6% and 10% contamination specimens, unlike the 20% contamination specimen in a more liquid state (Figure 7c).



**Figure 7.** Internal surface of specimens with 6% (a), 10% (b), and 20% (c) oil contamination.

### 3.3. Effect of Crude Oil on Relative Stiffness

The study investigated the rigidity (stiffness) of concrete samples with varying proportions of crude oil. The findings indicated a negative correlation between oil concentration and concrete stiffness (Figure 8). The concrete specimens subjected to a 1% oil assault had an average elasticity of 14 MPa/mm, marginally more significant than the control sample. However, a 20% oil assault reduced the specimens' stiffness by 77.5%. For specimens exposed to a 10% crude oil concentration, the stiffness decreased by 44.1%. Similarly, for specimens exposed to 2% and 6% crude oil concentrations, stiffness was reduced by 8.43% and 32.6%, respectively. As the oil content increases, the stiffness decreases in proportion to the slope of the first linear region. Hence, when the amount of sand in an oil assault exceeds 1%, the elastic limit of the concrete decreases, causing a greater extent of plastic deformation.

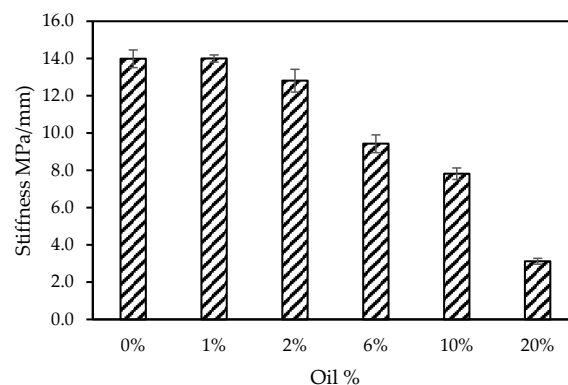


**Figure 8.** Mean stiffness of specimens with different oil content levels.

### 3.4. Influence of Crude Oil on Proportional Limit

Concrete design is significantly influenced by the proportional limit, which determines the highest stress that concrete can bear while still being able to recover to its original condition. When this limit is exceeded, plastic deformation is inevitable. Therefore, it is crucial to carefully consider the potential consequences of surpassing this restriction. The

behaviour of concrete is influenced by applied stresses, and the specimens contaminated with oil showed values that were 4.11% higher than those of the control sample when the crude oil contamination was 1% (Figure 9). There was a reduction of 10.75% in the limit when the crude oil percentage reached 10%, although the limit remained above 10 MPa. When the contamination levels approached 20%, the average limit decreased significantly to 2.77 MPa. Certain specific applications may find a proportional limit of 2.77 MPa sufficient [42,43]. Concrete with a compressive strength of over 10 MPa may be advantageous for constructing parking spaces, sidewalks, footpaths, and bus platforms [44,45].

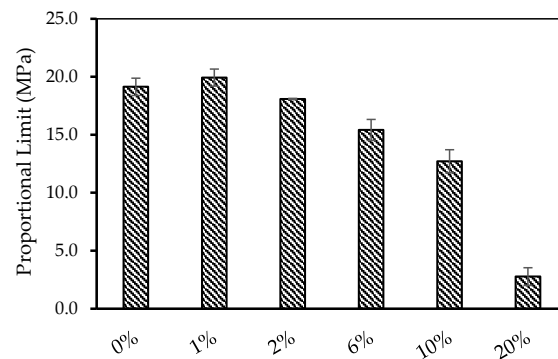


**Figure 9.** Mean proportional limit with different oil contents.

The average optimal strength for each oil content is compared to the average proportional limit in Figure 10. Risk is inherent in design when ultimate and proportional stresses are relatively similar because any exceedance of the service load may cause structural failure. The service load must be maintained below the proportional limit stress. However, using up to 6% oil-contaminated sand in concrete mixtures does not exceed the proportional limit stress. The study indicates that an ultimate measure of 10% oil contamination is appropriate for construction use. Nevertheless, as the oil content of the concrete reaches 20%, the concrete's physical characteristics are not practical for use. Oversaturation allows for excessive air voids, leading to significant concrete de-densification. As a result, concrete cannot be used structurally and further loses strength. Fibres can be added to concrete prepared with 10% oil-contaminated sand to address these shortfalls, again keeping below proportional limit stress. Fibres will work to bring back the concrete's structural integrity and general suitability.

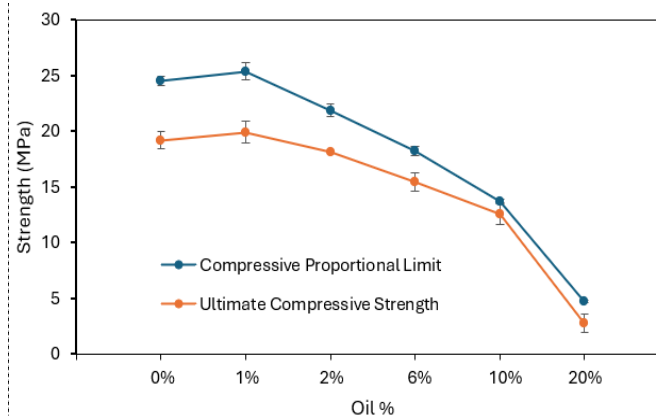


**Figure 10.** Comparison of average optimal strength with average proportional limit of specimens exposed to different oil contents.

### 3.5. Impact of Oil on the Hydration Process (Isothermal Calorimetry)

The heat flow curves of cement pastes with different crude oil contents were determined by isothermal calorimetry at 25 °C. Cement paste samples with varying percentages of crude oil content (0% to 20%) were used for the testing. Figure 11 shows the heat release

reaction demonstrating crude oil's impact on the cement paste's hydration process. It can be seen that 1% of crude oil does not impact the hydration process. Nevertheless, as crude oil increased beyond 1%, a delay in hydration and a reduction in the highest temperatures could be observed. This implies a slowdown in the hydration process. The study revealed that using 20% crude oil significantly affects the cement hydration process. The thermal profile obtained via isothermal calorimetry exhibited a suppression of the tricalcium silicate ( $C_3S$ ) peak and a significant reduction in the height of the third tricalcium aluminate ( $C_3A$ ) hydration peak [31]. At an early age, the cement hydration rate was faster for specimens with 0% and 1% crude oil contamination than those with 2% to 20% crude oil contents. The primary cement compounds, calcium silicates, play a crucial role in determining the final strength of the hardened cement paste. In detail, a high level of crude oil hindered the reaction of  $C_3A$  with water, which is typically very exothermic and forms calcium aluminate hydrate. This inhibition delayed  $C_3S$  and  $C_3A$  reactions, as can be seen in the thermal profiles. A high percentage of crude oil created a coating that impeded the reactions necessary for proper cement hydration. Ettringite, an insoluble calcium sulphoaluminate, formed more slowly around the  $C_3A$  particles. This made the hydration times longer and the physical bond between the cement paste and the aggregate weaker. Trezza and Scian [46] demonstrated that high levels of crude oil significantly impede tricalcium aluminate ( $C_3A$ ) hydration in the presence of water, a highly exothermic reaction that forms calcium aluminate hydrate.

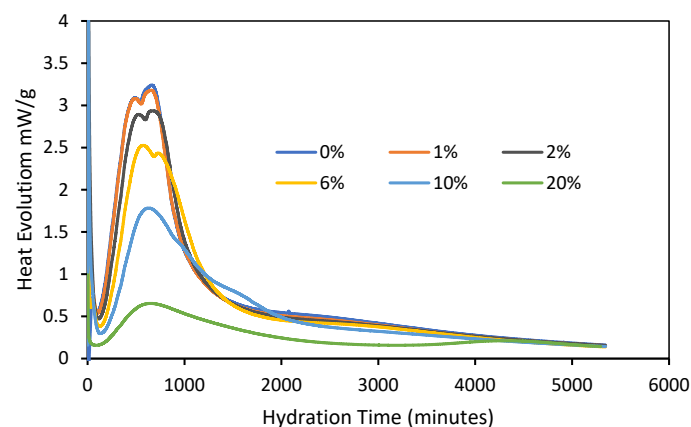


**Figure 11.** Effect of crude oil content on heat flow (mW/g).

Crude oil can interfere with the normal hydration process, altering the kinetics and formation of hydration products. However, a low level of crude oil contamination (1%) only partially affected the cement particles, as shown in Figure 12. This decreased the total surface area of the cement particles compared to the  $H_2O$  used ( $w/c$  ratio), which reduced the unreacted cement particles and consequently increased their mechanical properties.

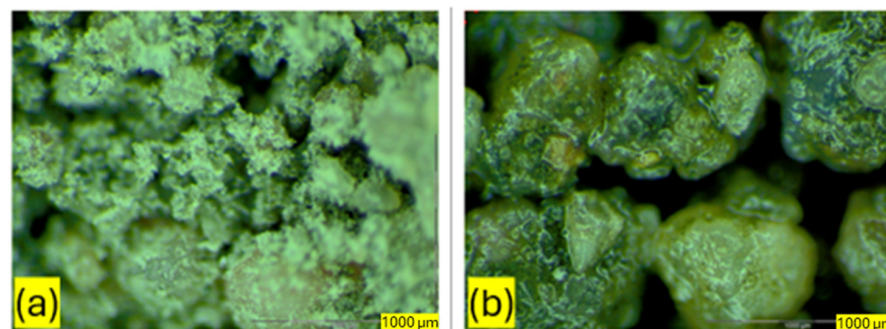


**Figure 12.** (a) Dry mix of cement and contaminated sand with 1% crude oil. (b) Dry mix of cement and contaminated sand with 20% crude oil.

Figure 13 presents the cumulative heat evolution of cement with varying crude oil contamination (0% to 20%), measured using an isothermal calorimeter. The results indicate that increased crude oil content decreases the cumulative heat values over 72 h. Specifically, at 1% crude oil content, there was no significant effect on cumulative heat evolution. Up to 24 h, the cumulative heats of the 0% and 1% contamination samples were identical. After 48 h, the cumulative heat of the 1% contamination sample decreased by less than 5 J/g compared to the control sample. However, higher levels of crude oil contamination (2% to 20%) significantly reduced the cumulative heat evolution. The maximum cumulative heat releases after 72 h for the 0% and 1% contamination samples were 1332.4 J/g and 1296.5 J/g, respectively. The cumulative heat releases for samples with 2%, 6%, and 10% crude oil contamination were 1248.1 J/g, 1146.4 J/g, and 959.4 J/g, respectively, gradually decreasing with increasing crude oil content. This reduction in cumulative heat evolution is supported by Almagro [19], who indicated that the presence of crude oil hinders the hydration reaction of cement, leading to decreased cumulative heat release. Specifically, the cumulative heat for samples with 20% crude oil contamination showed a significant reduction, reaching 60% of the control samples after 72 h, illustrating the inhibitory influence of crude oil on the hydration process of cement.

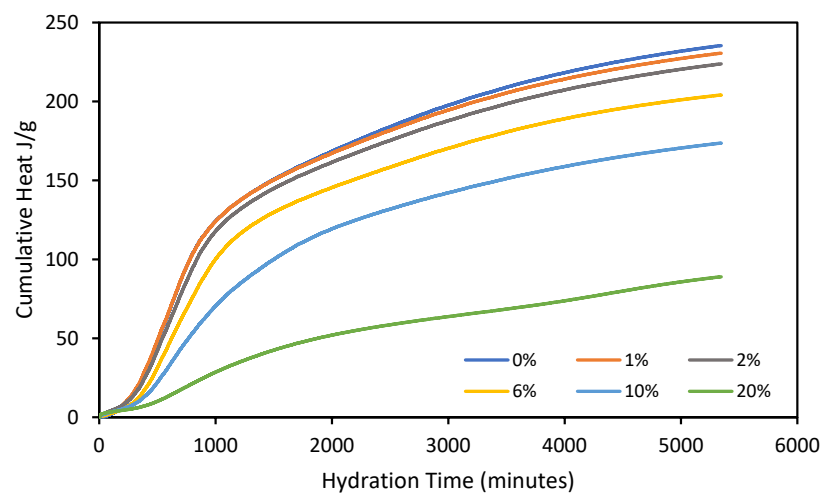


**Figure 13.** Effect of crude oil content on cumulative heat (J/g).

### 3.6. Properties of Fibre-Reinforced Oil-Impacted Concrete

#### 3.6.1. Compression Failure Mode of Fibre-Reinforced Oil-Impacted Concrete

The control and ReoShore 45 PP fibre-reinforced concrete specimens all displayed a splitting failure originating from the top cap, which propagated at a right angle to the load direction (Figure 14).



**Figure 14.** Comparison of failure modes of control samples (a) and ReoShore 45 samples (b).

Forta Ferro PP, steel, and glass fibre-reinforced concrete primarily exhibited shear failure (Figure 15). However, steel fibre-reinforced specimens demonstrated better crack control, narrower fracture widths, and less crumbling due to oil saturation compared to the other fibre types (Figure 15b).



**Figure 15.** Splitting failure of Forta Ferro PP fibre-reinforced samples (a) and steel fibre-reinforced samples (b).

Furthermore, examining fracture surfaces indicated that steel fibres have excellent dispersion and minimise tensile fractures (Figure 16a). On the other hand, the ReoShore 45 PP fibres shown in Figure 16b exhibit a horizontal alignment and intersecting tensile cracking. Still, their dispersion appears to be poor, as confirmed by inspection. Visual examination revealed an even distribution of Forta Ferro PP and glass fibres throughout the concrete.

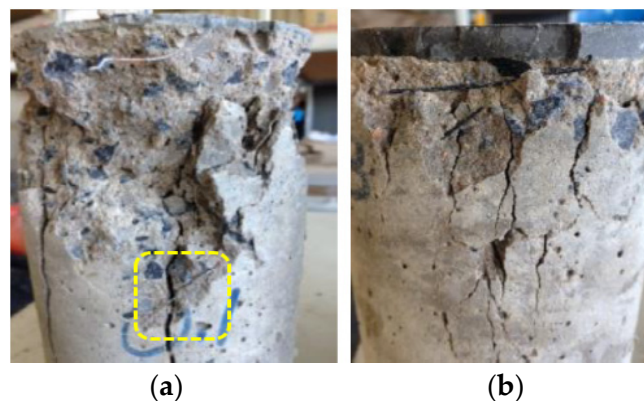


**Figure 16.** (a) Steel fibre- and (b) ReoShore 45 PP-reinforced sample failure surfaces.

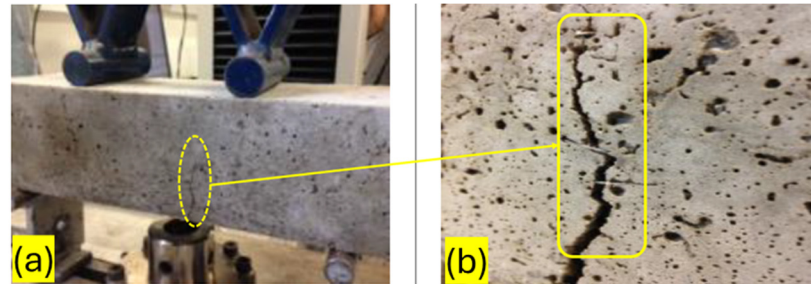
### 3.6.2. Flexural Failure Mode of Fibre-Reinforced Oil-Impacted Concrete

Research indicates that specimens with fibre reinforcement exhibit greater ductility to applied bending loads. In contrast, those without this reinforcement tend to experience substantial cracking in the centre surface, which results in structural failure (Figure 17a).



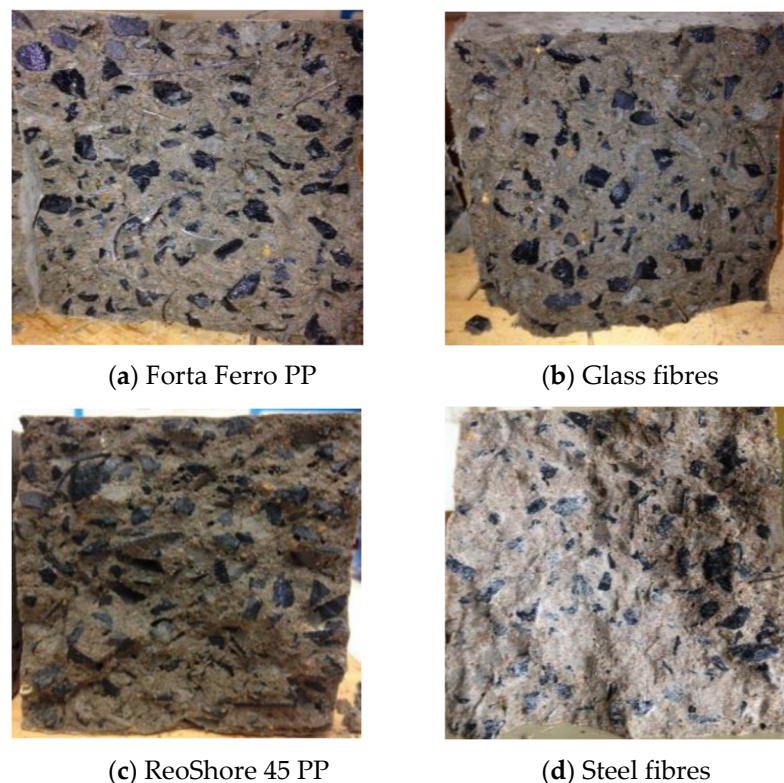
**Figure 17.** Failure behaviour in flexural tests: (a) control (10%), (b) FF, (c) PP, (d) GF, and (e) steel samples.

Figure 17b–e indicate that fibre reinforcement in the specimens resulted in a more gradual failure, characterised by reduced crack widths and less crack propagation, with some cracks originating from off-centre points. Compared to different fibres, steel fibre-reinforced concrete manifests the minimum propagation of tensile cracks, as shown in Figure 18. Across all FRC types, the reduced crack width implies effective crack bridging.



**Figure 18.** (a) Crack propagation process. (b) Connection of steel fibres with concrete.

Figure 19 illustrates the failure surfaces of flexural specimens. Among the fibres tested, glass fibres demonstrated the most effective dispersion, with a predominance of fibre orientation perpendicular to the failure plane, facilitating crack bridging. Forta Ferro PP fibres further revealed favourable dispersion, though they showed separation during casting. Conversely, ReoShore 45 PP fibres displayed deplorable dispersion, with only five fibres on the failure surface and just two oriented perpendicular to the failure plane. The steel fibres, dispersed randomly inside the matrix, were mainly oriented perpendicular to the surface where the failure occurred. These fibres played a crucial role in inhibiting the development of wider fractures.



**Figure 19.** Failure surfaces of flexural specimens: (a) distribution of FF fibres; (b) distribution of GF fibres; (c) distribution of PP fibres; (d) distribution of steel fibres.

### 3.6.3. Microscopic Analysis of Fibre-Reinforced Oil-Impacted Concrete

The bond between fibres and concrete was examined using microscopic techniques, determining the specimens' compressive and flexural behaviour. After testing, independent fibres were extracted for micro-extraction to examine the fibre–matrix bonds. Forta Ferro PP was found to be superior in its twisted-bundle formation. The fibre monofilament disintegrated into individual filaments, which blended with the concrete, forming a fibrillary structure that intertwines with the concrete particles. Figure 20 depicts the external bond between the filaments and the concrete, revealing the presence of air voids at the interface between the fibres and the concrete.



**Figure 20.** Microscopic images revealing the interaction between Forta Ferro PP fibres and the matrix.

The study found that, despite being the shortest, the glass fibres showed a high bonding ability with concrete due to their agglomerated fibrillated form, resulting in effective fibre–matrix interaction (Figure 21).



**Figure 21.** Glass fibre–matrix interaction (microscope images).

ReoShore 45 fibres rely on the design of their tread surface for anchorage to enhance the bond of these monofilaments with concrete. Voids can be observed around the fibre–matrix interface in Figure 22. The oil intensity across the top of the fibre might have compromised the anchorage of the fibre with the concrete.

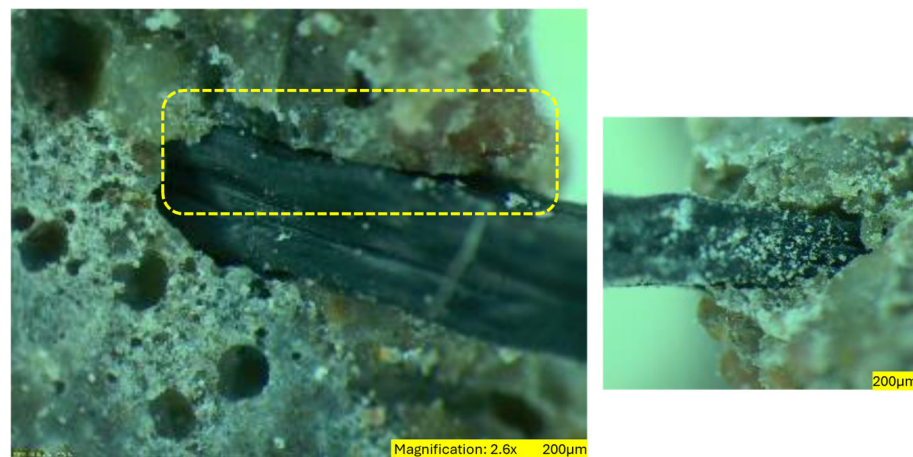


**Figure 22.** Microscope images of the interaction between ReoShore 45 and the matrix.

Steel fibres displayed a strong bond with concrete, as depicted in Figure 23. Figure 23, cement mortar firmly adheres to the steel fibre's surface, illustrating how mortar forms around the fibre without severances that could weaken the bond at the interface.



**Figure 23.** Microscopic images showing the interaction of steel with the matrix.

### 3.7. Effect of Fibres on Compressive Strength

Figure 24 illustrates the compressive strength of concrete contaminated with 10% oil, incorporating various fibres. The average strength of non-fibrous specimens with 10% crude oil is 13.79 MPa. Forta Ferro PP, glass, and steel fibre-reinforced concrete enhanced concrete strength by 27%, 28%, and 30%, respectively, compared to the control sample. On the other hand, the ReoShore 45 PP reinforcement increased concrete strength by an average of 15%.

Consistent with the findings reported by Døssland [29], Rai and Joshi [47], and Ezeldin and Balaguru [48], the results indicate that fibres have no discernible impact on compressive strength. Instead, steel fibres possess the most prominent characteristic that positively influences concrete strength. The resin-coated and hooked architecture significantly improved the bonding between the concrete matrix and the filler. In contrast, the rough surface of the ReoShore 45 PP fibre made it less effective in terms of energy dissipation during the compression behaviour of the fibres. According to the microscopic observations, the oil coatings on these fibres hampered their anchorage within the cement paste, resulting in poor energy dissipation, probably due to the insufficient elevation of the treads on the fibre surface (Figure 21). Additionally, analysis of failure behaviour revealed that specimens without fibres and those with ReoShore 45 PP, which exhibited minimal strength, displayed splitting failures. In contrast, steel, glass, and Forta Ferro PP fibre

specimens showed shear failure (Figures 14 and 15). From investigations by Markeset and Hillerborg [49], the presence of shear failure suggests that the fibres successfully handled the splitting of the material along its axis and that the failure occurred due to the interaction between axial fractures. Moreover, analysis of the compressive failure surfaces showed that the steel, glass, and Forta Ferro PP fibres had good dispersion within the concrete. Figure 18, in Section 3.6.2, illustrates the intersections between the tensile cracks in ReoShore 45 and the steel fibres. Löfgren [44] stated that the fibres crossing tensile cracks could restrain the lateral deformation of concrete in the compressed loading case. However, as the experimental results show, these intersections have a negligible influence on the compressive strength of concrete.

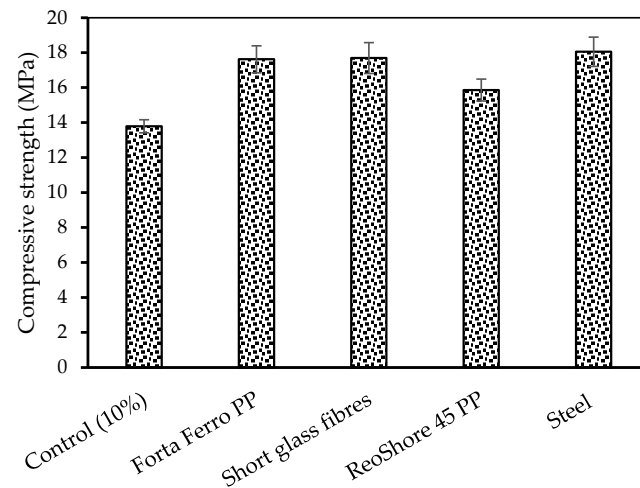


**Figure 24.** Compressive strength averages for specimens with various fibre types.

### 3.7.1. Effect of Fibres on Density

Figure 25 displays the average density of specimens for each type of fibre. A slight reduction in average density occurred in specimens comprising steel and glass fibres, with decreases of 0.10% and 0.11% observed. A negligible increase became evident in the specimens of ReoShore 45 PP fibre-reinforced concrete, with only a 0.01% increase in density compared to the control. In contrast, Forta Ferro PP fibres created a more pronounced increase in concrete density, averaging 0.27% compared to the non-fibrous specimen. Typically, the density of specimens reinforced with fibres does not differ from the density of non-fibrous specimens by more than 0.27%. This suggests that the quantity of fibres used in this experimental program did not primarily influence the concrete density of the specimens.

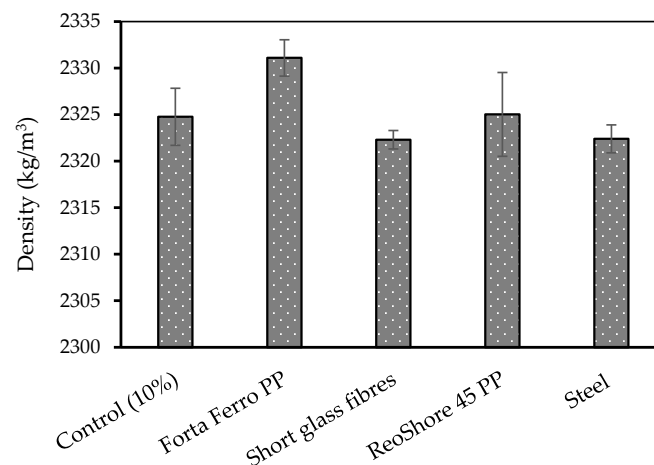


**Figure 25.** Average densities of specimens with different kinds of fibres.

### 3.7.2. Effect of Fibres on Stress–Displacement

The stress–displacement relationship of specimens is a crucial factor to consider when comparing different materials, especially in the case of fibre-reinforced concrete (FRC). Figure 26 displays a comparison of the stress–displacement curve for each form of fibre. The descending or softening branch of fibre-reinforced concrete (FRC) demonstrated enhanced performance as compared to standard concrete when combined with 10% crude oil. ReoShore 45 PP did not enhance the strength of the concrete, but it notably prolonged the weakening phase of the concrete after reaching its highest point. Both steel and Forta Ferro PP fibres indicated a displacement-softening post-peak behaviour that was more pronounced than that of ordinary concrete (with 10% crude oil). Consistent with the research conducted by Døssland [29], Ezeldin and Balaguru [48], Lee et al. [50], and Kooiman [51], the addition of fibres altered the failure mode of concrete, shifting it from a brittle state to a less brittle one. The observed behaviour in the data aligns with the pattern previously demonstrated by Löfgren [52], who concluded that fibres did not significantly alter concrete behaviour before reaching peak strength but that they did extend post-peak behaviour by mitigating lateral expansion and arresting the axial splitting failure plane. The stress-displacement relationship of specimens is a critical factor for comparison, especially for fibre-reinforced concrete (FRC). Figure 26 illustrates the representative stress-displacement curves for each fiber type. Compared to plain concrete with 10% crude oil, FRC demonstrated an improved softening or descending branch. Although ReoShore 45 PP did not enhance concrete strength, it notably extended the softening phase of the post-peak behavior. Both steel and Forta Ferro PP fibers also showed a more pronounced displacement-softening response after peak strength, relative to conventional concrete with 10% crude oil. This behaviour corroborates the findings of Døssland [29], Ezeldin and Balaguru [48], Lee, et al. [50] and Kooiman [51], indicating how the incorporation of fibres transitions the failure mode from brittle to more ductile. The observed results are consistent with Löfgren [52] conclusions, where fibers did not significantly affect concrete behavior before peak strength but extended the post-peak phase by reducing lateral expansion and preventing axial splitting failures.

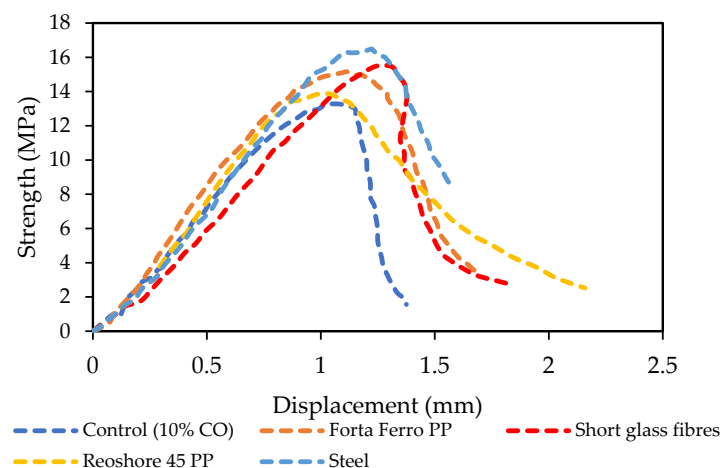


**Figure 26.** Stress–displacement relationships of samples with different types of fibres.

Furthermore, Forta Ferro PP, glass, and steel fibres led to increased displacement corresponding to the maximal stress of concrete. This aligns with the report documented by Maccaferri [28], who stated that a micro-scaffolding structure is formed by incorporating fibres with sufficient tensile strength and a uniform distribution in concrete. This structure effectively manages the concrete’s ductility, and the formation of fractures caused by shrinkage. Fibres play a crucial role in increasing the ductility of compressed concrete by preventing fractures and improving the energy required for cracks to form, a property that material scientists and engineers can appreciate.

### 3.7.3. Effect of Fibres on Relative Stiffness

Figure 27 depicts the average stiffness comparison between four different fibres and a control sample (10%). Forta Ferro PP, ReoShore 45 PP, and steel fibres increased the stiffness of concrete by 48.6%, 52.6%, and 13.4%, respectively. In contrast, glass fibres led to a 13.3% reduction in concrete stiffness from the control average.

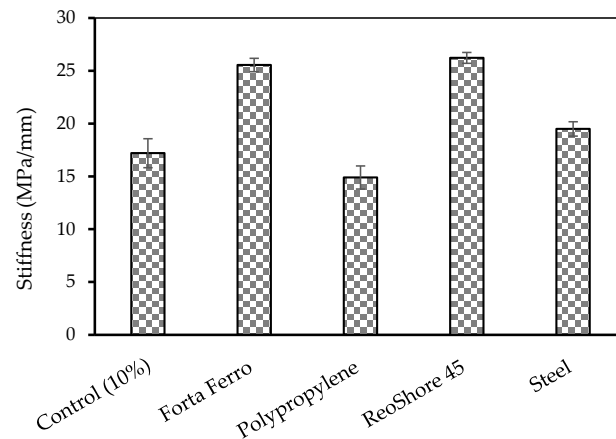


**Figure 27.** Average stiffness of specimens made with different types of fibres.

According to Beaudoin [53], a high fibre modulus of elasticity directly affects the matrix's elasticity by transferring stress from the matrix to the fibre. Nevertheless, the findings suggest that the very modest amount of fibre used did not significantly modify the elasticity of concrete. We attribute the discrepancy in the outcomes to the anticipated disparity across the various concrete compositions.

### 3.7.4. Effect of Fibres on Proportional Limit

Figure 28 illustrates the mean proportional limit of fibre-reinforced composite (FRC) from the stress–displacement graphs. In general, fibres enhanced the proportional limit of concrete. Forta Ferro PP fibre-reinforced concrete had the lowest proportional limit among the fibres examined. It showed a 9% increase compared to the control group's average, which consisted of plain concrete with 10% crude oil. The addition of ReoShore 45 PP to reinforced concrete resulted in a 12.3% increase in the proportional limit of the concrete, albeit slightly reducing its ultimate strength. Steel and glass fibres exhibited the highest enhancement in the proportional strength of concrete, with respective rises of 41.4% and 37.7% compared to plain concrete. Adding steel fibres to the concrete yielded a proportional strength of 14.68 MPa, which is close to the average proportional limit of 15 MPa found in concrete with 6% contamination.

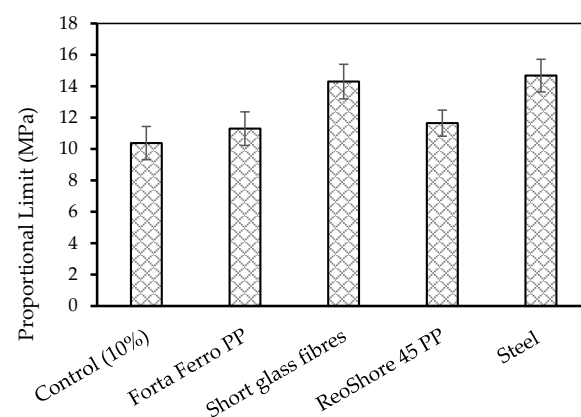


**Figure 28.** Mean proportional limits of specimens incorporating different fibre types.

### 3.8. Effect of Fibres on Flexural Strength

Figure 29 illustrates the ultimate flexural strength of FRC, showing that the average flexural strength of the non-fibrous control sample was 6.5 MPa. The inclusion of fibres was found to reduce the flexural strength of concrete affected by oil contamination. Specifically, the average reductions in strength for Forta Ferro PP, ReoShore 45 PP, and glass fibre reinforcements were 16.7%, 15%, and 6.6%, respectively, compared to the control samples with 10% oil contamination. Meanwhile, adding steel fibre reinforcement to concrete slightly enhanced its flexural strength by an average of 4.8%.

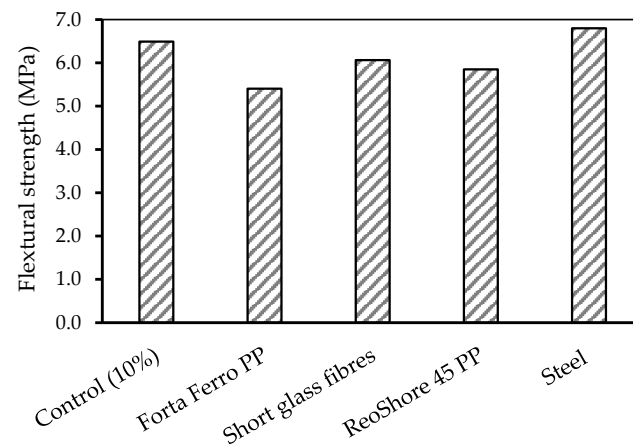


**Figure 29.** Typical flexural strengths of specimens with different fibre dosage amounts.

The results are consistent with the study by Alhozaimy et al. [54], which showed that adding glass fibres to concrete at doses below 0.3% by volume did not impact its flexural strength. The research found that Forta Ferro PP, glass, and ReoShore 45 PP fibres did not substantially improve the flexural strength of the concrete. This is because these fibres had lower tensile strengths than steel fibres and were added at a low dose of 0.1% by volume. In contrast, Wang and Wang [55] and Yazıcı et al. [56] noted that steel fibres significantly enhanced the flexural strength of concrete. The study examined the optimal fibre dosage of 0.5% by volume of concrete, which might have caused the little-observed enhancement. Microscopic analysis revealed that glass fibres and steel fibres demonstrated a strong bond with the concrete, as evidenced by a continuous fibre–matrix interface (Figure 24). In contrast, the examination of Forta Ferro PP and ReoShore 45 PP fibres revealed the presence of air voids around the fibre–matrix interface (Figures 22 and 24). Moreover, the ReoShore 45 PP fibres were visibly saturated with oil. Excessively oil-coated fibres are believed to have accumulated during the original investigation, thereby hindering the interaction between the fibres and the matrix.

### Effect of Fibres on Load–Displacement

Figure 30 displays the standard load–displacement correlation for each type of fibre. Excluding ReoShore 45 PP, the inclusion of these fibres enhanced the ductility of the concrete when subjected to flexural stress. Glass, Forta Ferro PP, and steel fibre-reinforced concrete exhibited greater displacements at failure loads of 0.7 mm, 1.0 mm, and 1.6 mm, respectively, due to the crack-bridging capabilities of the fibres. Figure 30 depicts the typical load–displacement relationships for every kind of fibre. All fibres, except ReoShore 45 PP, enhanced the ductility of the concrete when subjected to flexural pressure. The failure displacements of the fibres were 0.7 mm, 1.0 mm, and 1.6 mm for glass, Forta Ferro PP, and steel fibre-reinforced concrete, respectively.

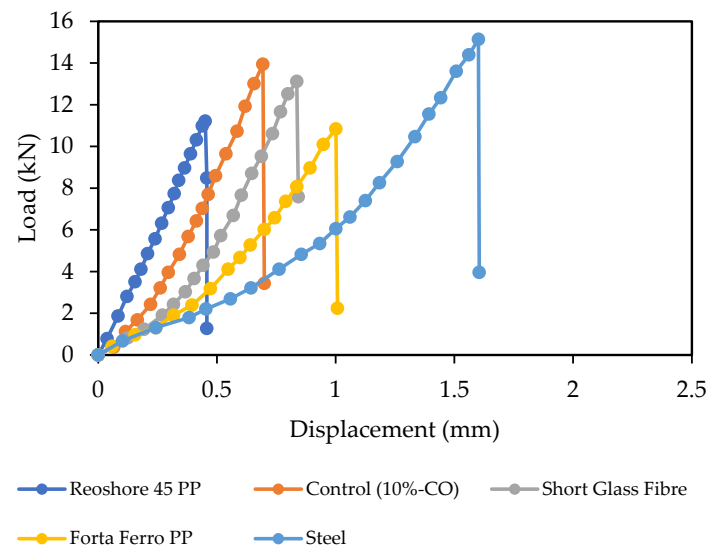


**Figure 30.** Flexural test of concrete (10%) with different fibre types.

Moreover, examination of FRC failure surfaces revealed that glass fibres and Forta Ferro PP fibres exhibited excellent dispersion along the failure plane, while steel fibres also showed good dispersion compared with ReoShore 45 PP fibres (see Figure 20). The steel fibres' high tensile strength and hooked shape enhanced the concrete's ductility. On the other hand, the even distribution of glass fibres and Forta Ferro PP fibres over the surface where failure occurs enabled effective load transfer when subjected to tensile stress.

Kooiman's [51] research revealed that fibres impact the softening behaviour of concrete through fibre bridging, resulting in a redistribution of stresses. Once cracking commences, stress redistribution establishes a new balance across the cross-section. Figure 17a shows that the non-fibrous specimens had abrupt failure near the middle, where the tensile stress is most crucial. The specimens reinforced with fibres did not break suddenly, but the cracks became smaller and sometimes started away from the centre because the tensile strength of the fibre-reinforced concrete was higher (Figure 17b–e). Steel and ReoShore 45 PP fibres, acting as monofilaments, enhance concrete's bond and mechanical qualities through their unique geometry and tensile strength. Conversely, the dispersal capacity and geometry of glass fibres and Forta Ferro PP fibres cause them to fibrillate. Oil saturation weakened the ReoShore 45 PP tread, reducing the bondability and limiting the ductility of the concrete (Figure 23). Furthermore, the failure surface revealed inadequate ReoShore 45 PP fibre dispersion along the flexural failure plane (see Figure 21). Examining the FRC failure surfaces revealed a well-spread distribution of glass and Forta Ferro PP fibres along the failure plane. Similarly, steel fibres were very well distributed compared to ReoShore 45 PP fibres (see Figure 19). The steel fibres' high tensile strength and hooked shape enhanced the ductility of the concrete. On the other hand, the glass fibres and evenly spread Forta Ferro PP fibres over the failure surface made it easier for load transfer under tensile stress.

### 3.9. Effect of Fibre Dosage on Oil-Impacted Concrete

#### 3.9.1. Influence of Fibre Dosage on Compression Failure Mode

Specimens with various doses of steel fibres mostly experienced shear failure. With an increase in the dose of fibres, the level of crumbling caused by oil saturation is reduced. Figure 31 shows the specimens with dosages of 0.1% and 0.5% after experiencing compressive failure. The lower-dosed specimens (a) exhibited a mix of splitting and conical failure. On the other hand, specimens with the greatest fibre dose exhibited a mix of shear failure and splitting failure with lower fracture widths (Figure 31b).

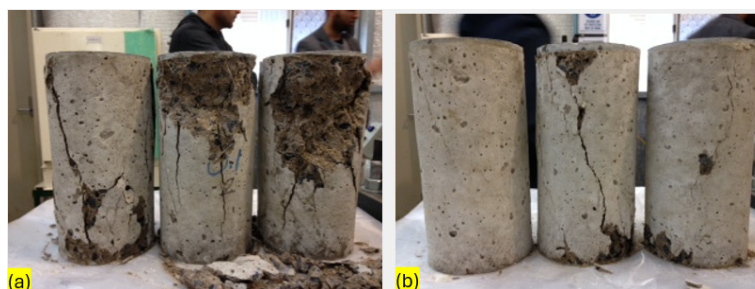


**Figure 31.** Compression failure modes: (a) 0.1%; (b) 0.5%.

### 3.9.2. Influence of Fibre Dosage on Flexural Failure Mode

With an increase in the dose of steel fibres, the breadth of cracks at the point of failure decreased. Figure 32 compares specimens with fibre volumes of 0.1% and 0.5% at the point of failure. Fracture propagation was much more successfully reduced at the highest dose of 0.5% than at the lowest dosage of 0.1%.

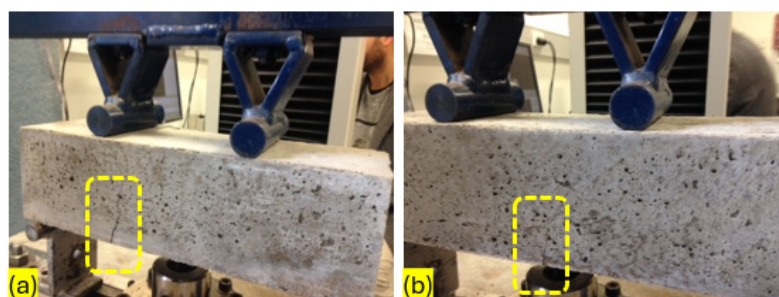


**Figure 32.** Flexural failure modes for 0.1% quantity (a) and 0.5% quantity (b).

The study of fractured surfaces revealed that fibre pull-out is the primary cause of failure. However, post-failure analysis showed that hooked ends still existed, suggesting that oil weakened the bond between the fibres and the concrete (Figure 33).



**Figure 33.** Pull-out failure (steel fibre).

### 3.9.3. Influence of Fibre Quantity on Workability

A slump test was carried out on each batch of fresh fibre dosages to compare the workability of oil-impacted concrete at various steel fibre dosages (Figure 34). In agreement with a study by Sarbini et al. [57], the findings indicate that the workability of concrete decreases as the amount of fibre added increases. Including fibres in the concrete resulted in a decrease in slump of 21%, 25%, 32%, and 46% compared to the lowest dose of fibres. The reduction in workability is linked to challenges in compacting concrete, impacting the likelihood of achieving evenly dispersed concrete [58].

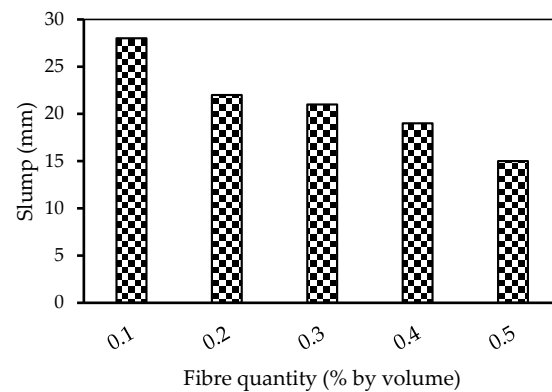


**Figure 34.** Slump vs. fibre quantities.

### 3.9.4. Effect of Fibre Quantity on Compressive Strength

The findings indicated that a fibre dose volume of 0.1% provided the maximum average compressive strength. An increase of 23.5% was observed at dosages of 0.1% when compared to the control average strength (concrete with 10% crude oil). However, the strength of fibre quantities surpassing 0.1% was only 13 to 14% higher than the non-fibrous average. In Figure 35, below, the red line displays the average compressive strength of non-fibrous concrete mixed with 10% crude oil and containing varying amounts of steel fibres. In alignment with the studies reported by Mansour et al. [59] and Hsu and Hsu [60], an increase in the dosage of steel fibres does not significantly enhance the compressive strength of concrete. Hsu and Hsu [60] indicated that increased fibre volume reduces workability in concrete, resulting in voids within the matrix and limiting strength enhancement, as shown in the slump results in Figure 34.

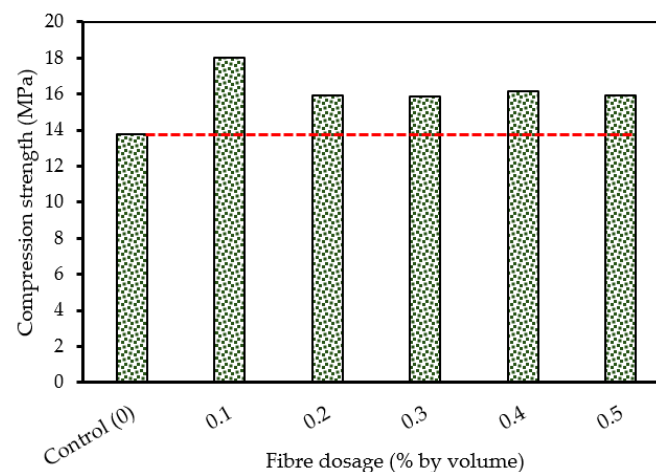


**Figure 35.** Influence of fibre quantities on compressive strength.

### 3.9.5. Effect of Steel Fibre Quantity on Stress Behaviour

Figure 36 compares the representative stress–displacement curves for different fibre dosage volumes. The research findings revealed that all the specimens exhibited ductile behaviour, extending the softening branch of concrete post-peak behaviour. On the other hand, increasing the fibre dose did not make the specimens less brittle after the peak. Instead, specimens with higher fibre volumes incurred increased displacements at failure load. The study conducted by Lee et al. [50] found that SFRC exhibited ductile behaviour after it reached a compressive failure load. Additionally, the displacement at this load typically increased in proportion to an increase in the fibre volume ratio. Figure 36 indicates that concrete with a 0.5% fibre volume ratio reached failure at 1.263 mm displacement, compared to 1.061 mm at the 0.1% fibre dosage. Moreover, the results on failure behaviour

(Figure 30) show that increasing the fibre volume reduces crack widths and crumbling due to saturation. This implies that increasing the fibre volume improves concrete ductility by lowering lateral deformation and increasing the energy needed for crack propagation.

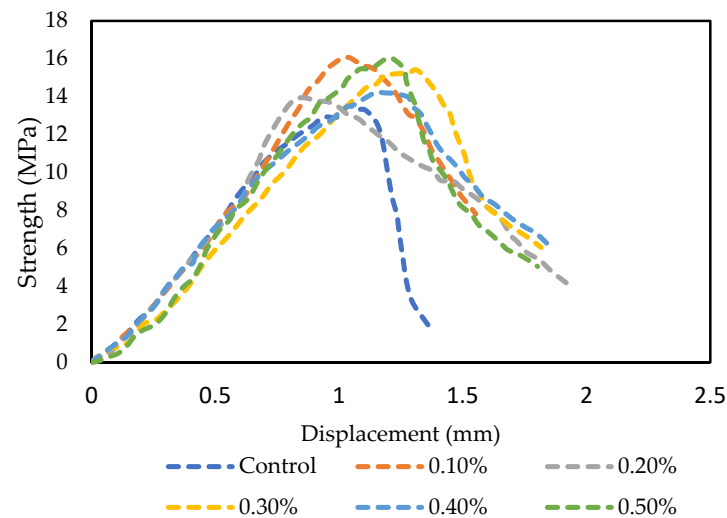


**Figure 36.** Stress–displacement interaction of compressive strength at varying steel fibre quantities.

### 3.9.6. Effect of Steel Fibre Dosage on Stiffness

Figure 37 shows the relative elasticity of specimens with 10% crude oil and different fibre dosages. The red horizontal line indicates the average stiffness of the control sample (10% oil), which is 7.8 MPa/mm. The results reveal that while the elasticity of concrete initially increases at low fibre dosages, it starts to decrease with higher steel fibre dosages. The minimum fibre dosage of 0.1% achieved the highest elasticity, showing a 46.8% improvement over the control average. However, the increase in fibre dosages from 0.2% to 0.5% did not show a significant increase in elasticity, and it varied between 38.5 and 45.1%. This reduction in elasticity is in agreement with the results of Neves and Fernandes de Almeida [61] and Rai and Joshi [47], who found that steel fibres slightly decreased concrete elasticity. Neves and Fernandes de Almeida [61] proposed that this reduction is due to fibres oriented parallel to the load acting as voids and that adding fibres increases the chance of this occurrence. Furthermore, the increased ductility from fibre addition, which leads to more gradual failure, might also reduce the concrete's elastic modulus.

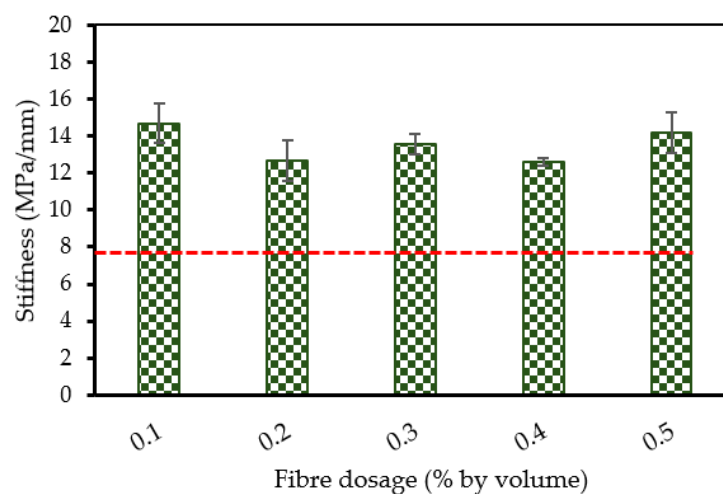


**Figure 37.** Average stiffness of samples with different quantities of steel fibres.

### 3.9.7. Effect of Steel Fibre Quantity on Proportional Limit

The mean proportional limits for various steel fibre dosages are illustrated in Figure 38. The red line indicates the average proportional limit for plain concrete with 10% crude oil. Steel fibre addition improved the proportional limit of oil-impacted concrete, but changes in fibre dosages had a minimal impact. The 0.1% fibre dosage achieved the highest proportional limit of 14.68 MPa. Other dosages resulted in only slight increases, from 3.7% at 0.3% to 8.2% at 0.1% compared to the average proportional limit of the control. A reduction of 0.6 was observed at 0.4% compared to the control sample. Despite the decrease in concrete elasticity caused by the inclusion of fibres, the proportional limit remained unaffected owing to the enhanced ductility of concrete. Nevertheless, a significant variation of up to 8.8% was seen across the different fibre doses tested, ranging from 0.1% to 0.5%. Therefore, it can be concluded that the dosage of steel fibres has a minimal impact on the proportional limit of concrete, primarily due to the voids introduced into the matrix as the fibre dosage increases. The volume of fibres has a more notable effect on the permanent deformation of the concrete.

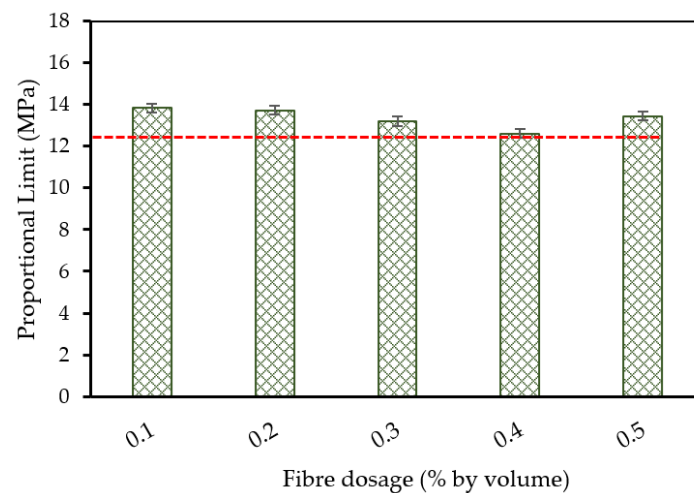


**Figure 38.** The average proportional limits of specimens with different steel fibre quantities.

### 3.9.8. Effect of Steel Fibre Quantity on Flexural Strength

Figure 39 illustrates how the amount of steel fibres impacts the bending strength of oil-impacted concrete. The red line denotes the average flexural strength of plain concrete with 10% oil contamination. The trend indicated that adding steel fibres nominally increases the flexural strength. The maximum strength improvement of 9.60% was observed with the highest fibre dosage of 0.5% by concrete volume. A 0.1% fibre dosage also improved strength by 4.78%. However, fibre dosages of 0.2%, 0.3%, and 0.4% showed a maximum strength increase of just 1.77% compared to the control average, with the 0.3% dosage yielding the most significant improvement. The difference in flexural strength between the lowest (0.1%) and highest (0.5%) fibre dosages was 0.71 MPa.

Similar findings were observed by Mansour et al. [59], Wang and Wang [55], and Yazıcı et al. [56]. It has been concluded that adding steel hooked-end fibres increased the concrete's flexural strength, and the findings showed that a softening reaction resulting from fibre bridging, which makes concrete more ductile, influences the increase in flexural strength. According to Figure 33, the analysis of flexural failure behaviour in concrete showed that fibres enhanced crack-bridging efficiency, reflected in the reduced crack widths and slower crack propagation at failure. Adding fibres increases the effectiveness of load transfer through crack bridging, as higher fibre volumes lead to more fibres bridging the failure path and thus improve concrete's tensile capacity. Despite this, the maximum increase in flexural strength achieved was only 0.62 MPa, or a 9.6% improvement with a 0.5% fibre dosage, which is a modest gain. The failure surface analysis (Figure 33) indicated that fibres generally maintained their hooked-end structure after failure. A strong

fibre–matrix bond leads to significant energy dissipation during fibre pull-out. However, the 10% crude oil contamination caused a substantial reduction in concrete density and strength, which is suspected to have diminished the fibres' ability to handle tensile stress and led to a bond-slip effect. This effect reduced the potential of steel fibres to enhance the concrete's flexural strength, resulting in only slight improvements.

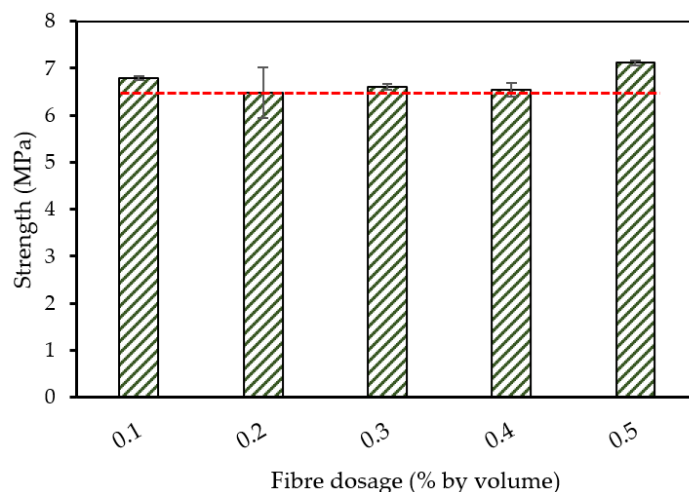


**Figure 39.** Comparison of average flexural strengths for specimens with different dosages of steel fibres.

#### 4. Conclusions

This research examined the effects of oil-contaminated sand and fibres on concrete properties. The findings led to the following conclusions:

**Oil Contamination Impact:** High percentages of oil-contaminated sand in concrete increase porosity and saturation, resulting in an 8.2% reduction in density at 20% crude oil contamination. Compressive strength decreases by 44% with 10% contamination and by 81% with 20% contamination compared to uncontaminated samples. However, 1% oil contamination improved compressive strength due to the oil's bonding effect with sand particles. Concrete with up to 10% contamination can still achieve a proportional limit above 10 MPa, making it suitable for various applications. Thus, 10% is considered the optimal maximum oil content for construction.

**Cement Paste Hydration:** Isothermal calorimetry analysis revealed that 1% crude oil does not affect hydration, but higher levels slow the process. At 20% crude oil, there is a significant suppression of the tricalcium silicate peak and a reduction in the height of the third tricalcium aluminate peak, indicating that high oil levels impede proper cement hydration and weaken the bond between cement paste and aggregate.

**Effect of Fibres:** The fibres did not significantly alter the physical properties or density of oil-impacted concrete but improved compressive strength by 30%. Steel fibres were the most effective, increasing flexural strength by 4.8% compared to the non-fibrous average. All the fibres except ReoShore 45 PP enhanced concrete ductility by increasing displacement at failure loads. However, matrix saturation reduced the effectiveness of crack bridging.

**Steel Fibre Performance:** Adding steel fibres to concrete with 10% crude oil contamination did not enhance compressive strength but decreased elasticity in compression and increased ductility during permanent deformation. Nonetheless, steel fibres improved flexural strength, with a maximum enhancement of 9.6% achieved with the 0.5% steel fibre dosage. Saturation reduced fibre pull-out resistance, limiting crack-bridging effectiveness. The optimal fibre volume dosage improved flexural strength while decreasing compressive strength.

Overall, the study found that utilising 10% oil-contaminated sand delayed the fibres' ability to stabilise cracks and transfer loads, which typically enhances concrete

strength. Consequently, adding fibres had a minimal impact in terms of improving the mechanical properties of concrete with 10% crude oil contamination. High percentages of oil-contaminated sand should be used in low-strength applications. Further research is needed to determine the maximum oil contamination level that retains the benefits of short fibres and to explore methods for mitigating reductions in mechanical properties.

**Author Contributions:** Conceptualisation, R.A. and F.A.; methodology, R.A.; formal analysis, F.A., R.A., O.A. and A.A.; investigation, F.A., R.A. and O.A.; writing—original draft preparation, A.A., O.A. and F.A.; review and editing, F.A. and R.A.; funding acquisition, F.A., O.A. and A.A. All authors have read and agreed to the published version of the manuscript.

**Funding:** The research was funded by Prince Sattam bin Abdulaziz University through the project number PSAU/2024/01/99513.

**Institutional Review Board Statement:** Not applicable.

**Informed Consent Statement:** Not applicable.

**Data Availability Statement:** Data are contained within the article.

**Acknowledgments:** The authors thank Prince Sattam bin Abdulaziz University for funding this research work through the project number PSAU/2024/01/99513.

**Conflicts of Interest:** The authors declare no conflicts of interest.

## References

- Tomassi, A.; Caforio, A.; Romano, E.; Lamponi, E.; Pollini, A. The development of a Competence Framework for Environmental Education complying with the European Qualifications Framework and the European Green Deal. *J. Environ. Educ.* **2024**, *55*, 153–179. [CrossRef]
- Fazioli, R. *Economic Analysis and Evaluations of Natural Gas Hydrates Exploitation by Injection of CO<sub>2</sub>: Hydrate-Based Carbon Capture Technologies*; Tab Edizioni: Rome, Italy, 2024.
- Cames, M.; Graichen, J.; Kasten, P.; Kühnel, S.; Faber, J.; Nelissen, D.; Shanthi, H.; Scheelhaase, J.; Grimme, W.; Maertens, S. Climate protection in aviation and maritime transport: Roadmaps for achieving the climate goal. *Proj. Rep.* **2023**, *26*, 1–243.
- Chevron Corporation 2023. Purpose Powers Progress. Available online: <https://www.chevron.com/-/media/chevron/annual-report/2023/documents/2023-Annual-Report.pdf> (accessed on 15 July 2024).
- Casey, K. *The Coming Chaos: Fossil Fuel Depletion and Global Warming*; Dorrance Publishing: Pittsburgh, PA, USA, 2018.
- Shayuti, M.S.M.; Zainal, S.; Ya, T.M.Y.S.T.; Abdullah, M.Z.; Shahrudin, M.Z.; Othman, N.H.; Alias, N.H.; Mohd, T.A.T.; Sharudin, R.W. Assessment of contaminants in sand production from petroleum wells offshore Sabah. *Environ. Sci. Pollut. Res.* **2023**, *30*, 17122–17128. [CrossRef]
- Li, X.; Wang, X.; Ren, Z.J.; Zhang, Y.; Li, N.; Zhou, Q. Sand amendment enhances bioelectrochemical remediation of petroleum hydrocarbon contaminated soil. *Chemosphere* **2015**, *141*, 62–70. [CrossRef]
- Johnston, J.E.; Lim, E.; Roh, H. Impact of upstream oil extraction and environmental public health: A review of the evidence. *Sci. Total Environ.* **2019**, *657*, 187–199. [CrossRef]
- Saborimanesh, N. Toward sustainable remediation of oil sands fine Tailings—A review. *J. Environ. Manag.* **2021**, *288*, 112418. [CrossRef]
- Ordinioha, B.; Brisibe, S. The human health implications of crude oil spills in the Niger delta, Nigeria: An interpretation of published studies. *Niger. Med. J.* **2013**, *54*, 10–16. [CrossRef] [PubMed]
- Kadafa, A.A. Oil exploration and spillage in the Niger Delta of Nigeria. *Civ. Environ. Res.* **2012**, *2*, 38–51.
- Mees, E. Ras Lanuf Extinguished After Seven Days. In *Middle East Economic Survey*; Middle East Petroleum and Economic Publications (Cyprus) Ltd.: Nicosia, Cyprus, 2008; Volume 51, p. 35.
- Abousnina, R.; Manalo, A.; Lokuge, W.; Al-Jabri, K.S. Properties and structural behavior of concrete containing fine sand contaminated with light crude oil. *Constr. Build. Mater.* **2018**, *189*, 1214–1231. [CrossRef]
- Aryee, A. Risks of Offshore Oil Drilling: Causes and Consequences of British Petroleum Oil Rig Explosion. *Aquat. Sci. Technol.* **2013**, *1*, 17. [CrossRef]
- Jalaei, F.; Zoghi, M.; Khoshand, A. Life cycle environmental impact assessment to manage and optimize construction waste using Building Information Modeling (BIM). *Int. J. Constr. Manag.* **2021**, *21*, 784–801. [CrossRef]
- Guerin, T.F. Tactical problems with strategic consequences: A case study of how petroleum hydrocarbon suppliers support compliance and reduce risks in the minerals sector. *Resour. Policy* **2021**, *74*, 102310. [CrossRef]
- Maleki, M.; Kazemzadeh, Y.; Dehghan Monfared, A.; Hasan-Zadeh, A.; Abbasi, S. Bio-enhanced oil recovery (BEOR) methods: All-important review of the occasions and challenges. *Can. J. Chem. Eng.* **2024**, *102*, 2364–2390. [CrossRef]

18. Srouf, I.; Chong, W.K.; Zhang, F. Sustainable recycling approach: An understanding of designers' and contractors' recycling responsibilities throughout the life cycle of buildings in two US cities. *Sustain. Dev.* **2012**, *20*, 350–360. [CrossRef]
19. Almabrok, M.; McLaughlan, R.; Vessalas, K. Characterisation of cement mortar containing oil-contaminated aggregates. In *Proceedings of the Australasian Conference on the Mechanics of Structures and Materials*; CRC Press/Balkema: Leiden, The Netherlands, 2013.
20. Abousnina, R.; Manalo, A.; Ferdous, W.; Lokuge, W.; Benabed, B.; Saif Al-Jabri, K. Characteristics, strength development and microstructure of cement mortar containing oil-contaminated sand. *Constr. Build. Mater.* **2020**, *252*, 119155. [CrossRef]
21. Almabrok, M.; McLaughlan, R.; Vessalas, K. Evaluating the effect of mixing method on the performance of mortar containing oil. *Int. J. Eng. Sci. Invent.* **2015**, *4*, 58–64.
22. Ajagbe, W.O.; Omokehinde, O.S.; Alade, G.A.; Agbede, O.A. Effect of crude oil impacted sand on compressive strength of concrete. *Constr. Build. Mater.* **2012**, *26*, 9–12. [CrossRef]
23. Abousnina, R.M.; Manalo, A.; Shiao, J.; Lokuge, W. Effects of Light Crude Oil Contamination on the Physical and Mechanical Properties of Fine Sand. *Soil Sediment Contam. Int. J.* **2015**, *24*, 833–845. [CrossRef]
24. Oluremi, J.R.; Osuolale, O.M. Oil contaminated soil as potential applicable material in civil engineering construction. *J. Environ. Earth Sci.* **2014**, *4*, 87–99.
25. Abousnina, R.; Alsalmi, H.I.; Manalo, A.; Allister, R.L.; Alajarmeh, O.; Ferdous, W.; Jlassi, K. Effect of Short Fibres in the Mechanical Properties of Geopolymer Mortar Containing Oil-Contaminated Sand. *Polymers* **2021**, *13*, 3008. [CrossRef]
26. Maddah, M.; Bencheikh, V. Properties of concrete reinforced with different kinds of industrial waste fiber materials. *Constr. Build. Mater.* **2009**, *23*, 3196–3205. [CrossRef]
27. Yuhazri, M.; Zulfikar, A.; Ginting, A. Fiber reinforced polymer composite as a strengthening of concrete structures: A review. *IOP Conf. Ser. Mater. Sci. Eng.* **2020**, *1003*, 12135. [CrossRef]
28. Maccaferri. Fibers as Structural Element for the Reinforcement of Concrete. 2015. Available online: <http://maccaferribalkans.com/al/docs/documents/broshura/fibers.pdf> (accessed on 20 May 2024).
29. Døssland, Å.L. Fibre Reinforcement in Load Carrying Concrete Structures: Laboratory and Field Investigations Compared with Theory and Finite Element Analysis. Ph.D. Thesis, Norwegian University of Science and Technology, Trondheim, Norway, 2008.
30. Khan, M.; Abbas, Y.; Fares, G. Review of high and ultrahigh performance cementitious composites incorporating various combinations of fibers and ultrafines. *J. King Saud Univ.-Eng. Sci.* **2017**, *29*, 339–347. [CrossRef]
31. Abousnina, R.; Manalo, A.; Lokuge, W.; Zhang, Z. Effects of light crude oil contamination on the physical and mechanical properties of geopolymer cement mortar. *Cem. Concr. Compos.* **2018**, *90*, 136–149. [CrossRef]
32. AS 1141.11.1; Methods for Sampling and Testing Aggregates—Particle Size Distribution—Sieving Method. Standards Australia: Sydney, Australia, 2009. Available online: <https://pdfcoffee.com/as-1141111-2009-methods-for-sampling-and-testing-aggregates-particle-size-distribution-sieving-method-pdf-free.html> (accessed on 20 May 2024).
33. AS 1726; Geotechnical Site Investigations. Standards Australia: Sydney, Australia, 1993. Available online: <https://pdfcoffee.com/1726-australian-standard-pdf-free.html> (accessed on 20 May 2024).
34. Simetric. Specific Gravity of Liquids. Available online: [http://www.simetric.co.uk/si\\_liquids.htm](http://www.simetric.co.uk/si_liquids.htm) (accessed on 20 May 2024).
35. Guideline, D. Design of Concrete Structures—Steel wire fibre reinforced concrete structures with or without ordinary reinforcement. *Infrastruct. Het Leefmilieu Dep. Leefmilieu Infrastruct.* **1995**, *4*, 227–239.
36. Naaman, A.E. Engineered steel fibers with optimal properties for reinforcement of cement composites. *J. Adv. Concr. Technol.* **2003**, *1*, 241–252. [CrossRef]
37. ASTM C1231; Standard Practice for Use of Unbonded Caps in Determination of Compressive Strength of Hardened Cylindrical Concrete Specimens. ASTM: West Conshohocken, PA, USA, 2014; Volume 4.
38. ASTM C1609; Standard Test Method for Flexural Performance of Fiber-Reinforced Concrete (Using Beam with Third-Point Loading). ASTM: West Conshohocken, PA, USA, 2019.
39. Osuji, L.C.; Ezebuoro, P.E. Hydrocarbon contamination of a typical mangrove floor in Niger Delta, Nigeria. *Int. J. Environ. Sci. Technol.* **2006**, *3*, 313–320. [CrossRef]
40. Lee, S.-Y.; An, J.; Kim, J.; Kwon, J.-H. Enhanced settling of microplastics after biofilm development: A laboratory column study mimicking wastewater clarifiers. *Environ. Pollut.* **2022**, *311*, 119909. [CrossRef]
41. Umar, A.; Ghosh, S.K. Effect of Oil Contamination on the Properties of Concrete. *J. Mater. Civ. Eng.* **2012**, *24*, 629–634. [CrossRef]
42. Abousnina, R.M.; Manalo, A.; Lokuge, W.; Shiao, J. Oil Contaminated Sand: An Emerging and Sustainable Construction Material. *Procedia Eng.* **2015**, *118*, 1119–1126. [CrossRef]
43. Spence, R.D.; Shi, C. *Stabilization and Solidification of Hazardous, Radioactive, and Mixed Wastes*; CRC Press: Boca Raton, FL, USA, 2004.
44. Fragomeni, S.; Venkatesan, S. *Incorporating Sustainable Practice in Mechanics and Structures of Materials*; CRC Press: Boca Raton, FL, USA, 2010.
45. Sriravindrarajah, R.; Do, H.; Nguyen, L.; Aoki, Y. Effect of clogging on the water permeability of pervious concrete. In *Incorporating Sustainable Practice in Mechanics and Structures of Materials*; Fragomeni, S., Venkatesan, S., Eds.; Taylor & Francis Group: London, UK, 2011.
46. Trezza, M.; Scian, A. Waste fuels: Their effect on Portland cement clinker. *Cem. Concr. Res.* **2005**, *35*, 438–444. [CrossRef]
47. Rai, A.; Joshi, Y. Applications and properties of fibre reinforced concrete. *J. Eng. Res. Appl.* **2014**, *4*, 123–131.

48. Ezeldin, A.S.; Balaguru, P.N. Normal-and high-strength fiber-reinforced concrete under compression. *J. Mater. Civ. Eng.* **1992**, *4*, 415–429. [[CrossRef](#)]
49. Markeset, G.; Hillerborg, A. Softening of concrete in compression—Localization and size effects. *Cem. Concr. Res.* **1995**, *25*, 702–708. [[CrossRef](#)]
50. Lee, S.-C.; Oh, J.-H.; Cho, J.-Y. Compressive behavior of fiber-reinforced concrete with end-hooked steel fibers. *Materials* **2015**, *8*, 1442–1458. [[CrossRef](#)]
51. Kooiman, A.G. *Modelling Steel Fibre Reinforced Concrete for Structural Design*; Springer: Singapore, 2000.
52. Löfgren, I. *Fibre-Reinforced Concrete for Industrial Construction*. Ph.D. Thesis, Chalmers University of Technology, Göteborg, Sweden, 2005.
53. Beaudoin, J.J. *Handbook of Fiber-Reinforced Concrete: Principles, Properties, Developments and Applications*; William Andrew: Norwich, NY, USA, 1990.
54. Alhozaimy, A.; Soroushian, P.; Mirza, F. Mechanical properties of polypropylene fiber reinforced concrete and the effects of pozzolanic materials. *Cem. Concr. Compos.* **1996**, *18*, 85–92. [[CrossRef](#)]
55. Wang, H.; Wang, L. Experimental study on static and dynamic mechanical properties of steel fiber reinforced lightweight aggregate concrete. *Constr. Build. Mater.* **2013**, *38*, 1146–1151. [[CrossRef](#)]
56. Yazıcı, Ş.; İnan, G.; Tabak, V. Effect of aspect ratio and volume fraction of steel fiber on the mechanical properties of SFRC. *Constr. Build. Mater.* **2007**, *21*, 1250–1253. [[CrossRef](#)]
57. Sarbini, N.N.; Ibrahim, I.S.; Saim, A.A. Enhancement on strength properties of steel fibre reinforced concrete. In Proceedings of the 3rd International Conference European Asian Civil Engineering Forum (EACEF) Conference, Yogyakarta, Indonesia, 20–22 September 2011.
58. Lamond, J.F.; Pielert, J.H. *Significance of Tests and Properties of Concrete and Concrete-Making Materials*; ASTM International: West Conshohocken, PA, USA, 2006; Volume 169.
59. Mansour, F.R.; Parniani, S.; Ibrahim, I.S. Experimental study on effects of steel fiber volume on mechanical properties of SFRC. *Adv. Mater. Res.* **2011**, *214*, 144–148. [[CrossRef](#)]
60. Hsu, L.S.; Hsu, C.T. Stress-strain behavior of steel-fiber high-strength concrete under compression. *Struct. J.* **1994**, *91*, 448–457.
61. Neves, R.D.; Fernandes de Almeida, J. Compressive behaviour of steel fibre reinforced concrete. *Struct. Concr.* **2005**, *6*, 1–8. [[CrossRef](#)]

**Disclaimer/Publisher’s Note:** The statements, opinions and data contained in all publications are solely those of the individual author(s) and contributor(s) and not of MDPI and/or the editor(s). MDPI and/or the editor(s) disclaim responsibility for any injury to people or property resulting from any ideas, methods, instructions or products referred to in the content.